Proceedings World Geothermal Congress 2015
Melbourne, Australia, 19-25 April 2015

The Potential of Hydrothermal Flames to Induce Spallation in Gneiss

T. Meier, D. Brkic, M. J. Schuler, M. Kant, Ph. Rudolf von Rohr

ETH Zurich, Institute of Process Engineering, Sonneggstrasse 3, 8092 Zurich, Switzerland

meier@ipe.mavt.ethz.ch

Keywords: Geothermal Energy, Hydrothermal Spallation Drilling, Drilling Technology, Heat Transfer

ABSTRACT

Despite the great potential of geothermal electricity production, its exploitation is hindered by the cost particularities and the high initial investment risks of the respective projects. In most geothermal power production projects, nearly 15% of the total investment costs are spent in a high risk period. Exploration, test drilling and the actual production drilling account between 40-70% of the total costs of a geothermal power plant, and 25% of it is spent during the high risk period of the project [1]. These facts call for alternative drilling technologies, in order to make geothermal electricity production sustainable. Spallation drilling is a technique that could reduce the drilling costs for geothermal electricity production. It takes advantage of the properties of certain rock types, to spall them into small disk-like fragments. Hydrothermal flames can be used in water-filled boreholes exceeding the critical pressure of water to provide the required heat to spall the rock. The work presented in this paper focuses on preliminary results towards the development of a drilling tool in a novel high pressure (260 bar) pilot plant. The impingement temperature profiles along the centerline of the pressure vessel are presented. Preliminary drilling experiments in rock probes (83 mm diameter - 150 mm length) follow and the flame impingement heat transfer is finally characterized. The heat flux serves to interpret drilling experiments and as a design parameter for further development. This procedure will be repeated until the drilling tool is optimized for a certain rock type.

1. INTRODUCTION

The current share of geothermal in the European renewable electrical grid is about 1.5% and is expected to decrease to 1.15% towards 2020 [2]. One condition to reverse this tendency and exploit its great potential is the reduction of the drilling cost. According to a study from Gehringer et al. [1] the risks related to a geothermal power plant are decreased greatly at the end of the drilling test period. Furthermore exploration, test drilling and the well drilling itself account up to 70% of the total investment for a geothermal power plant.

Gathering the data for the cost of completed wells as a function of depth from the oil and gas industry, Tester et al. [3] showed the exponential increase of well costs with depth. This increase can be directly related to the wear out of conventional drilling bits in the hard polycrystalline rock layer present in the earth's crust at depth of 4 to 5 km. This rapid wear out induces lower penetration rates and requires frequent replacement of the drilling head. Beside the intrinsic cost of the spare parts, the trip time necessary to exchange the head can become prohibitive.

Thermal spallation is a contact-free drilling technique ([4], [5], [6] and [7]) using a flame-jet to induce thermal stresses in a rock specimen. If the compressive stress field is intense enough, the pre-existing flaws of most hard polycrystalline rock will combine, grow and eventually fail. The high penetration rates demonstrated by this technique led to its industrial exploitation for more than three decades ([5], [8]). Unfortunately due to a sharp increase of the fuel price, the difficulties to excavate the cuttings and to sustain the borehole stability using gaseous drilling fluids, the exploitation of the spallation rigs stopped.

In the mid-80s, the technical progresses allowed the ignition of flames in a supercritical water-like environment (hydrothermal flames). The use of flames in water permits to utilize conventional drilling fluids and therefore solves the problems related to cuttings excavation and well stability. Owing to the heat transfer properties of supercritical water, hydrothermal flames seem to be promising to generate the required heat flux for spallation.

To investigate the potential of hydrothermal spallation drilling a pilot plant was built at the Institute of Process Engineering, ETH Zurich [9]. It allows to simulate the harsh – temperature and pressure – conditions expected in a geothermal well.

2. EXPERIMENTAL SETUP

The experimental setup used in this study occupies a space of 70 m^3 on two levels. It consists of four main fluid networks leading to a pressure vessel (Figure 1). Two high pressure plunger pumps ensure redundancy of the cooling water, a triple head metering membrane pump pressurizes the fuel as two gas boosters pressurize the oxygen. Two electrical heaters serve to preheat the fuel - an aqueous ethanol mixture - and the oxygen streams before their mixing and subsequent ignition. A surface ignition module described in [10] allows reliable forced ignition.

The outlet of the combustion chamber features two concentric annuli, the inner space (Ø =10 mm) accelerates the hydrothermal flame in the main volume of the pressure vessel as the intermediate one allows to inject the cooling water (**Error! Reference source not found.**). The circular water curtain leaves the combustion chamber diverging from the centerline by 45°.

The pressure is adjusted to 260 bar by throttling a triple stem needle valve. The effluent stream leaving the pressure vessel is mixed with the cooling water provided by one water plunger pump to cool down the mixture below its flash point before the pressure reduction step.

The pressure vessel (**Error! Reference source not found.**) consists of two concentric cylinders separated by a cooling mantle. Twelve holes perforated in the inner cylinder allow to balance the pressure between the two volumes. Within the internal cylinder the stem of a linear actuator serves to move either a plate with ten thermocouples laser-welded on its surface, a heat flux sensor or a rock probe.

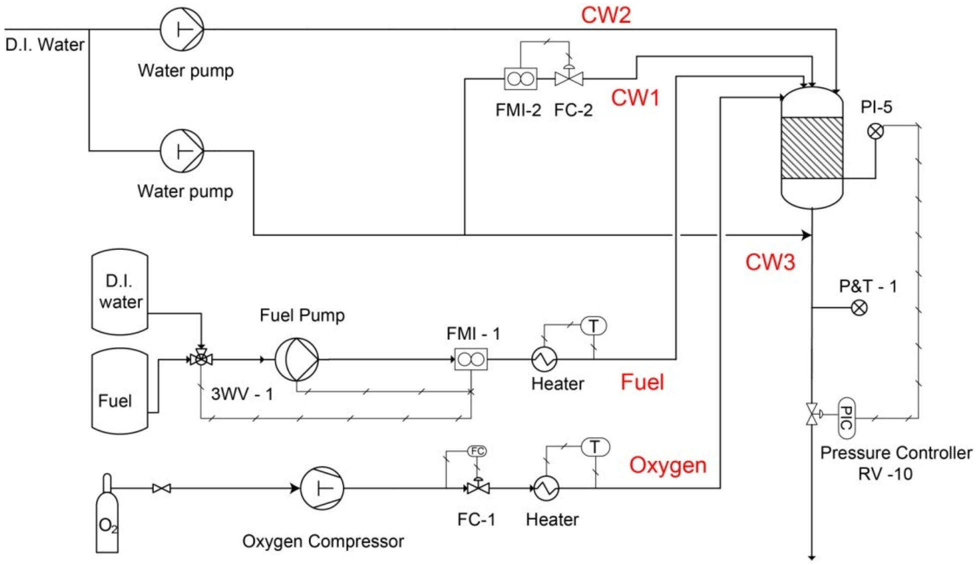

Figure 1 : Simplified process and instrumentation diagram of the experimental setup. The cooling water 1 and 2 (CW1, CW2) as well as the oxygen plus fuel network lead to the pressure vessel. The main equipment relevant to each network are labelled in the figure.

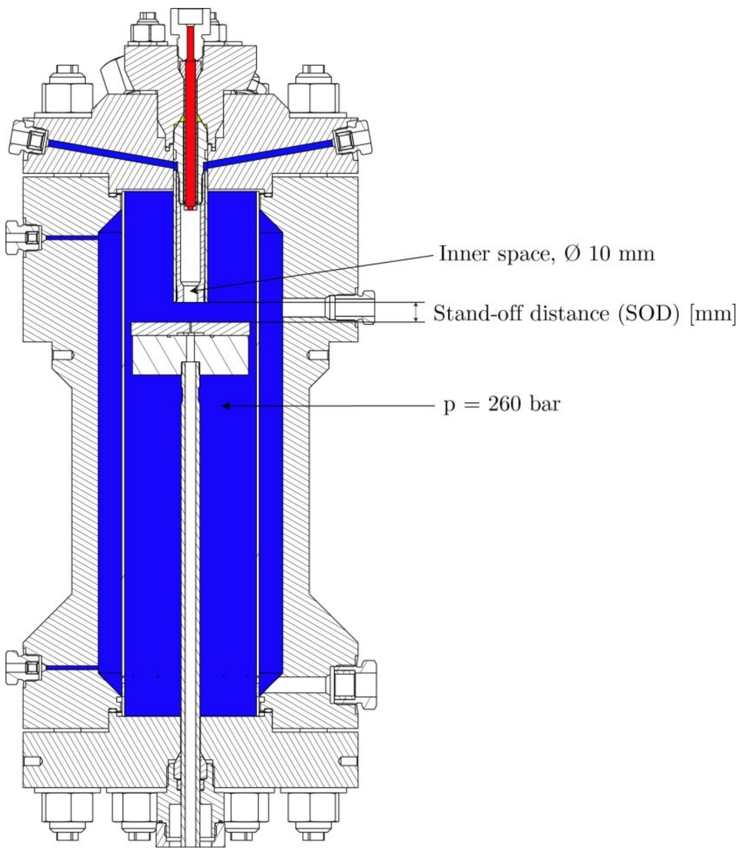

Figure 2: Pressure vessel used in this study equipped with the thermocouple plate. The space filled with cooling water is depicted in blue, the space filled by fuel is depicted in red and the space filled by oxygen is depicted in yellow.

The thermocouples are positioned such that they form three equidistant radii (Figure 3) of a circle covering a surface of 180 mm^2 centered on a circular plate (Figure 3) covering 6360 mm^2. The heat flux sensor covers an area of 35 mm^2 and is located in the center of the plate. It is based on the transverse Seebeck effect and therefore responds to a temperature gradient both in the axial and radial direction. The granitic rock probe has a cylindrical shape featuring a diameter of 83 mm and a length of 150 mm. The distance between the outlet of the combustion chamber to the sensor, respectively to the rock probe is denoted hereafter as stand-off distance (SOD).

Further details concerning the design and the construction of the pilot plant are available in [9].

3. RESULTS

The data presented in this paper are measured at four different operating points. The preheating temperatures of the oxygen stream (250°C) and the fuel stream (410°C) plus the oxygen to fuel ratio (λ = 1.2 with respect to stoichiometry) are kept constant throughout the experiments. The other relevant process parameters are presented in Table 1.

Table 1: Process parameters describing the different operating points used for the measurements. The fuel mass flow and its ethanol content define its nominal power.

Fuel [kg/h] (m_f)	Ethanol mass fraction [-] (x_{EtOH})	Fuel power [kW]	Combustion chamber cooling water [kg/h] (C_W)
60	17.5	78	350
60	17.5	78	475
60	15	67	350
50	17.5	65	350

The results are divided in three different sections. First the temperature profiles of ten K-Type thermocouples laser-welded on a plate as a function of the distance from the combustion chamber outlet are presented. The second section presents the heat flux produced by a flame featuring a thermal power of 78 kW. In the last section, the preliminary drilling experiments are presented together with the expected axial temperature profile in the center of the rock probes at relevant times.

3.1 Oblique impingement temperature profiles

The temperature profiles measured as a function of the stand-off distance are shown in Figure 3-5. Every measurement is performed during at least 60 seconds with a sampling rate of 1 Hz. Afterwards the time averaged value of each thermocouple is computed.

The symbols depict the space averaging temperatures over the ten thermocouples as the error bars represent the statistical fluctuation between the thermocouples. They show how concentrated the jet-flame is as a function of the stand-off distance.

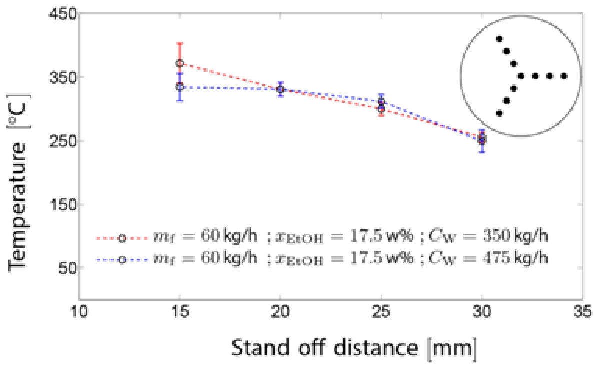

Figure 3 : Influence of the cooling mass flow.

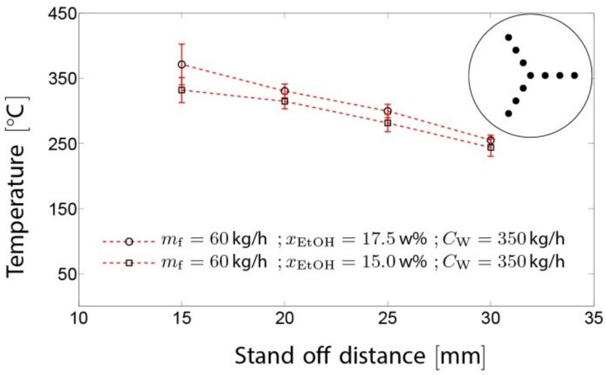

Figure 4 : Influence of the fuel concentration.

Figure 3 shows the effects of the cooling mass flow rate. The influence of the cooling increases monotonically towards the combustion chambers as the water curtain impinges closer to the thermocouple array. Figure 4 presents the effect of the ethanol mass fraction on the impingement temperature profiles. The ethanol content of the fuel mixture shifts the impingement temperatures to higher values as the fuel mass flow (Figure 5) has a limited effect on the impingement temperature.

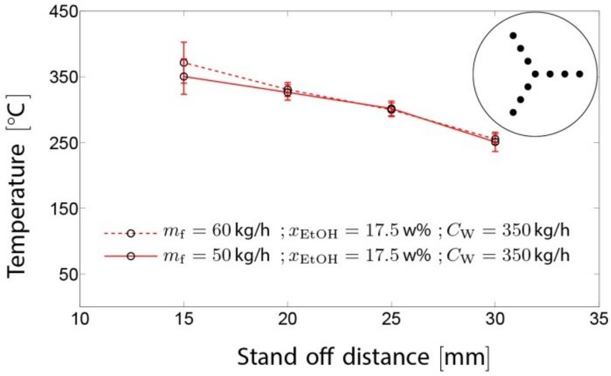

Figure 5 : Influence of the fuel mass flow.

3.2 Impingement heat transfer

The heat flux produced by an hydrothermal flame with a thermal power of 78 kW is measured using a transient heat flux sensor embedded in a plate itself mounted on the stem of the linear actuator. The measurements for two stand-off distances are presented in Figure.

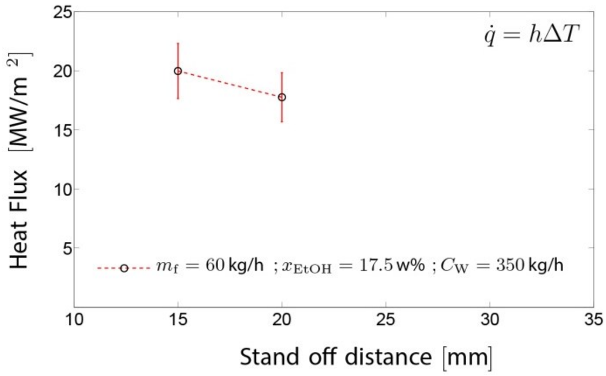

Figure 6 : Heat flux measured on a flat surface at relevant distances from the combustion chamber. The uncertainty is in the order of 11%.

Because of the intrinsic thermodynamic properties of supercritical water, the heat flux produced by hydrothermal flames are large at respectively low - flame to surface - temperature difference. In order to extrapolate the temperature and heat flux measurements to the rock surface, a correction for the different thermal conductivities between the rock and the sensors has to be performed. Without this correction, the heat flux to the rock is overestimated and the rock surface temperature underestimated.

In any case, such hydrothermal flame seems to fulfill the conditions required to initiate spallation in terms of heat flux (~1 MW/m^2) and surface temperature (~500°C) as stated by Rauenzahn [11].

3.3. Preliminary rock drilling experiments

The rock samples presented in Figure 7 were subjected to the hydrothermal flame conveying a thermal power of 78 kW at a stand-off distance of 15 mm for increasing time from left to right (1, 10, 30 min). The mass flow of cooling water through the combustion chamber was set to 350 kg/h for consistency with former experiments.

In Figure 7 a slight increase of the cavity size raising the exposure time from 1 to 10 min is shown. However, the process is not continuous as no obvious difference are present between 10 and 30 min of exposure.

In the rock probes number 2 and 3 (exposure time 10 and 30 min) the surface silica grains are oxidized over a circular area covering ~700 mm^2. Therefore the planar confinement requiring less than 10% of the surface of an unconfined sample to be heated up [6] was not fulfilled anymore and the stresses released [6].

3.4. Axial temperature profile along the rock centerline

The axial temperature profiles are relevant to gain insight in the state of stress within the rock assuming the planar confinement criteria [6] is fulfilled. As a matter of fact, if the rock is considered homogeneous and isotropic, the induced stress distribution is directly proportional to the temperature gradients. Although these assumptions do not reflect the reality perfectly, they provide a qualitative insight in the state of stress.

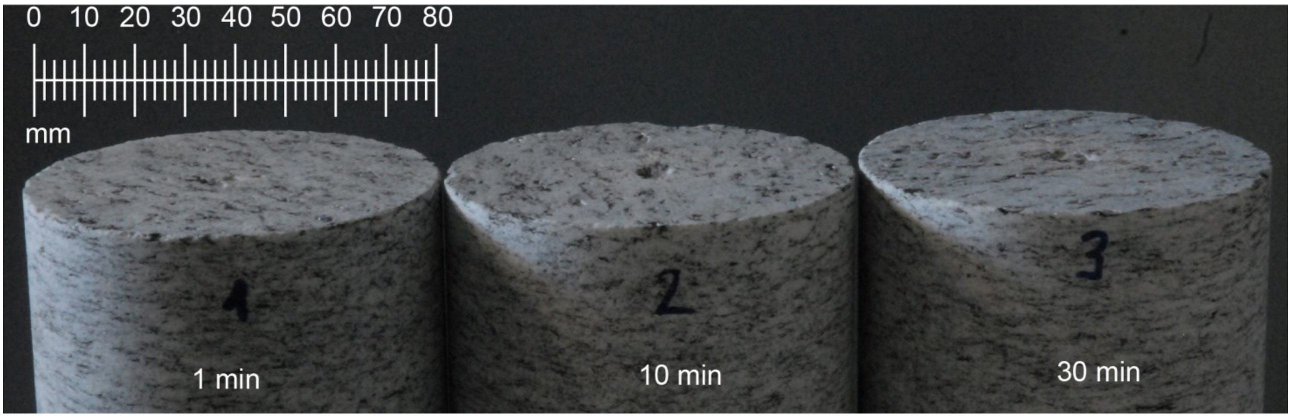

Figure 7 : Rock probes after different exposure time at a distance of 15 mm away from the combustion chamber. The exposure time is from left to right : 1, 10, 30 minutes. The thermal power of the flame is 78 kW and the mass flow of cooling water exiting the combustion chamber is 350 kg/h.

In Figure the temperature distributions along the centerline of the rock probes are presented. As it does not evolve anymore after 10 minutes the rock is therefore saturated by the hydrothermal flame. Furthermore the state of stress in the rock probe starts to decreases as the temperature profile flattens. Browning et al. [4] reported the penetration rates as a function of the incident heat flux. If the heat flux is too low, the induced stress field is not strong enough to fracture the rock. In contrary, if the heat flux is too high, the heat diffuses faster than the spalls are removed, the temperature profile flattens and the stresses are diminished. Therefore, an optimal incident heat flux must exist for every kind of rock.

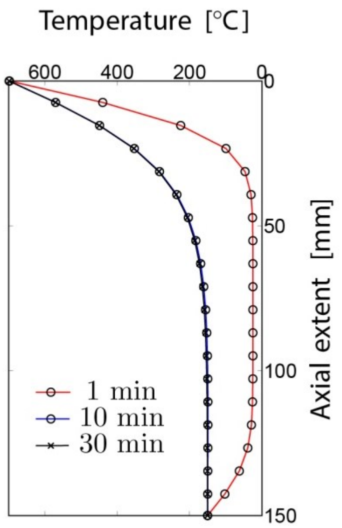

Figure 8 : Temperature profile as a function of the axial extent of the rock probe for three different relevant times.

4. CONCLUSION

The results presented in this paper are encouraging for the future development of a hydrothermal spallation drilling bit. However, in order to make use of the efficiency of the process, the thermal confinement condition has to be fulfilled in order to ensure a confinement of the rock probe intense enough. This condition is not easily achieved in the lab as the rock sizes are limited.

In the future development of the spallation drilling bit, we will try to concentrate the heat and find the optimum heat flux to drill the gneiss samples. Nevertheless, the results presented in this study prove the feasibility of spallation drilling with hydrothermal flames.

REFERENCES

[1] M. Gehringer and V. Loksha, "Geothermal handbook : Planning and financing power generation," tech. rep., Energy Sector Management Assistance Program and The World Bank, June 2012.

[2] E. Commission *et al.*, "Renewable energy: Progressing towards the 2020 target," *January 2011*, 2011.

[3] J. W. Tester, B. Anderson, A. Batchelor, D. Blackwell, R. DiPippo, E. Drake, J. Garnish, B. Livesay, M. C. Moore, K. Nichols, *et al.*, “The future of geothermal energy: Impact of enhanced geothermal systems (egs) on the united states in the 21st century,” *Massachusetts Institute of Technology*, 2006.

[4] J. Browning, W. Horton, and H. Hartman, “Recent advances in flame-jet working of minerals, 7th symp,” *Rock Mech., Pennsylvania State Univ., University Park*, 1965.

[5] J. J. Calaman and H. C. Rolseth, “Jet piercing,” *Transactions of the American Institute of Mining, Metallurgical and Petroleum Engineers*, pp. 325–337, 1968.

[6] W. M. Gray, “Surface spalling by thermal stresses in rocks,” in Proc. Rock Mechanics Symposium. Toronto, published by Dept. of Mines and Tech. Surveys, Ottawa, Jan, vol. 15, pp. 85–105, 1965.

[7] K. Thirumalai, “Process of thermal spalling behavior in rocks an exploratory study,” in The 11th US Symposium on Rock Mechanics (USRMS), 1969.

[8] W. C. Rea, “Method of and apparatus for quarrying and shaping rock and stone,” Mar. 22 1938. US Patent 2,111,872.

[9] P. Stathopoulos, Hydrothermal Spallation Drilling Experiments in a Novel High Pressure Pilot Plant. PhD thesis, ETH Zurich, 2013.

[10] P. Stathopoulos, K. Ninck, and P. R. von Rohr, “Hot-wire ignition of ethanol-oxygen hydrothermal flames,” Combustion and Flame, vol. 160, no. 11, pp. 2386 – 2395, 2013.

[11] R. M. Rauenzahn, Analysis of rock mechanics and gas dynamics of flame-jet thermal spallation drilling. PhD thesis, Massachusetts Institute of Technology, 1986.